Estimating the Prospects of Wave Energy Potential in Eastern Mediterranean using Multi-mission Satellite Altimeter Data

Maria Kaselimi and Demitris Delikaraoglou

National Technical University of Athens, Dept. of Surveying Engineering,
Heroon Polytechnioy 9, Zografou 15780, Athens, Greece.
maria.kaselimi@hotmail.com, ddeli@mail.ntua.gr

Abstract: Nowadays, the imbalance between availability, demand, and production capacity of energy resources, coupled with the impacts of climate change and of fossil fuels-related ecological risks make the future energy resources planning, management, and decision-making a challenging process. This has lead to the need for coming up with insightful strategies to facilitate the transition to cleaner energy resources, such as solar, wind and wave energy. Specifically, exploitation of wave energy requires three basic levels of decisions: assessing the offshore wave energy potential and detecting the most energetic coastal areas, selecting appropriate type of wave-energy-converters (WEC) and lastly, optimally distributing the captured wave energy to the power network. In this paper, we focus on how the exploitation of wave energy fits into the future energy landscape in the Eastern Mediterranean. Using multi-mission satellite altimetry-derived measurements of significant wave height allowed us to identify several possible locations of wave parks in the offshore areas of Greece and Cyprus. From the levels of wave size, period and energy density, it was then made possible to recommend an appropriate WEC type, based on practical considerations including wave directionality, structural complexity and ease of access for WEC maintenance etc.

Key words: satellite altimetry, significant wave height, wave energy

1. Introduction

In the context of global trends, nowadays, the exploitation of renewable energy resources is considered as an issue of major importance. Fossil fuels-based (coal, oil, and natural gas) non-renewable resources are insufficient to support growing economies and largely responsible for significant environmental pollution problems. Even nuclear power which once seemed quite promising is now slowly being abandoned due to concerns about safety, accidental risks and the cost of the disposal of radioactive waste. Furthermore, the rapid changes due to global warming, ocean acidification and climate change are powerful incentives so as to focus on expanding the usage of renewable energy resources for economic growth.

Wave energy is one form of abundant and widely available, harmless renewable resource with an enormous global potential. For that reason, the scientific and investment communities have turned their attention to it as it has numerous potential advantages: it is predictable and easy to estimate the amount of energy that it can produce; it affords a variety of ways to harness it; it creates no damage or has minimal negative environmental effects to the land and ocean environments where the wave energy converter installations are placed; and, it does not produce greenhouse emissions or waste products. However, wave energy has still to overcome a number of technological hurdles relative to other renewable energy technologies, notably that: offshore wave power farms may cause conflicts with other coastal endeavors such as tourism, fishing activities, shipping lanes, etc. and hence prevent local acceptance or raise questions about preserving the biodiversity and ecosystem goods and services. Furthermore, at least up to now, the costs of wave power generation installations and their maintenance are generally thought to be still quite high, although future costs are expected to drop significantly as larger facilities would be up and running.

Initial discussion for converting wave energy into a useable form of energy began in the late 17th century, but up to 1973 only a few attempts were made for producing wave energy. An early device that later became known as *Oscillating Water Column* (OWC) was first invented around 1940 and used operationally in Japan since 1965 and later in the US (Falcão, 2010). In the mid-70′s, support for renewable oceanic (tidal, current, thermal and wave) energy was increased due to the oil shortage and rising oil prices. However, the first industrial developments in wave energy technologies were soon abandoned by the early 1980′s, since they were regarded as immature, diverging, and not proven on a commercial scale and, hence, considered as operationally non-profitable. As a consequence, the interest for the production of energy from the oceans returned into experimental laboratories where various wave energy devices were eventually invented and thoroughly tested. Consequently, the experience gained from previous failed attempts, and relevant knowledge gained in the meantime from the mining and oil production technologies in the marine environment eventually led to developments of new generation power installations for the oceans. Specific to wave energy exploitation there were several studies that mainly drew attention to the need of careful selection of appropriate locations where favorable wave conditions prevail, such as duration, size and intensity of waves, spatial and temporal variations, etc. Such were, for instance, the coastlines facing the Eastern Atlantic which are traditionally identified as regions with high wave energy potential. Thus, countries such as Spain and Portugal have, with government support, developed and tested several utility-scale wave power installations at appropriate locations for wave farms (Iglesias et al., 2011). Recently, similar studies concerning the Eastern Mediterranean by Ayat (2013) and Zodiatis et al. (2014) identified specific locations off the coasts of Cy-

prus and Israel that were deemed suitable for the installation of wave farms, especially in view that in those areas other significant activities of sea energy exploitation (e.g. oil extraction, gas, desalination, etc.) are currently being planned or already taking place.

A first coordinated attempt to quantitatively assess the offshore European wave energy potential was done using the third generation wave analysis model (WAM) in the context of the European Wave Energy Atlas –WERATLAS Project (Pontes et al., 1996). Clement et al. (2002) reported that Greece, with its approximately 16.000 km of coastline, has high wind potential over the Aegean Sea that induces relatively strong constant wave activity, with an annual mean wave power projected at 4-11 kW/m. Furthermore, as strong reflection and diffraction phenomena of waves occur in this region, the exploitable wave energy potential of Greece is considered the highest in the Mediterranean, estimating that it amounts to about 5-9 TWh of electricity that can be generated annually. Naturally, such levels of wave energy if appropriately harvested, could contribute significantly to the power needs of many of the islands in the Aegean, especially the non-interconnected ones.

In retrospect, however, from both the systematic quality control of the WERATLAS data products and the prognostic capability studies of the underlying WAM model (Soukisian and Prospathopoulos, 2003) it has been shown that, in this area, the WERATLAS and WAM models tend to underestimate the significant wave heights (SWH) in a systematic way. This has been also verified from limited earlier comparisons with altimeter data from the TOPEX/Poseidon satellite and wave data from the Hellenic POSEIDON Network of buoys in the Aegean Sea, although the noted correlations between these models and data types is nevertheless quite high. With these preliminary findings in mind, this present study, as a follow-up of the preliminary findings by Delikaraoglou[2] (2012), was set out to show that using multi-year, multi-mission altimetry-derived wave data is particularly advantageous in assessing the wave energy potential of areas with relatively low steady wave heights over most of the year, such as in the broader Eastern Mediterranean region. Briefly stated, one can use the fact that each time an altimetry satellite passes from offshore to nearshore, it practically measures instantaneous profiles of SWH, albeit rather coarse in spacing, from which various wave related quantities can be reliably calculated and monitored at various locations of interest, thus allowing to produce useful maps depicting the offshore and nearshore wave energy statistics for entire maritime regions.

2. Data and Methodology Used

Wind waves, or wind-generated waves, are wrinkles that occur on the surface of open waters due to air pressure variations and shear effects caused by the blowing

wind. Enclosed seas such as the Mediterranean, the Baltic, and the Black Sea are considered almost free of tides and the wind is the main cause of the observed formation of waves on their surface.

Assuming an ideal sinusoidal wave, its total (kinetic plus dynamic) energy is dependent on the length of the wave and the square of wave height and given by the following simple equation:

$$E = E_K + E_D = \frac{1}{2}\rho g a^2 \lambda = \frac{1}{8}\rho g H^2 \lambda \quad (1)$$

where ρ = 1025 kg/m^3 is the seawater density, g = 9.81 m/s^2 is the gravity acceleration, H and a are respectively the height and width of the wave (in m), and λ (also in m) is the length of the wave. An important indicator for assessing the wave energy potential is the energy density of waves (in J/m^2 or Wh/m^2) which is defined as the ratio of energy to the length of the wave:

$$E_{dens} = \overline{E} = \frac{E}{\lambda} = \frac{1}{8}\rho g H^2 \quad (2)$$

Energy density reflects the mean energy of the entire length of a wave, whereas wave power P is equal to the rate of work (i.e., the transfer or absorption of energy) being produced. It can be shown that, in deep water, where the water depth is larger than half the wavelength, the wave power transmitted by a wave front passing through a vertical plane perpendicular to the direction of motion of the wave is given by the so-called *deep water force relationship*:

$$P = E_{dens} * c_g = \frac{\rho g^2 H^2 T}{32\pi} \quad (3)$$

where c_g is the wave's group velocity (in m/s) and T (in s) is the period of the wave motion. Turning to random waves, the previous relationship can be expressed in terms of the so-called *significant wave height* (denoted, in the literature, as *SWH* or H_s or $H_{1/3}$) representing the average wave height (trough to crest) of the highest one-third of the waves observed, and based on the relationship:

$$H_s = \frac{(1/N)}{3}\sum_{i=1}^{N} H_i \quad (4)$$

where N is the number of waves in a sample ordered from highest to lowest. In practice, most wave-measuring devices estimate *SWH* from a wave spectrum, relating H_s to the zeroth-order moment (area) of the wave spectrum or spectral wave height H_{m0} and the square root of the average of the squares of all wave heights, symbolically H_{rms}, through the relationship $H_{1/3} \cong H_{m0} = \sqrt{2}\, H_{rms}$. Consequently, the deep water force relationship can also be expressed as

$$P = \frac{\rho g^2 H_{rms}{}^2 T}{32\pi} = \frac{\rho g^2 H_{m0}{}^2 T}{64\pi} = \frac{\rho g^2 H_s{}^2 T}{64\pi} \cong 0.5 H_s{}^2 T \quad (5)$$

Respectively, satellite radar altimeters are designed to measure the return power of a radar pulse that is reflected off the ocean surface. They are unique in measuring directly the *SWH* from the different times of return from wave crests and troughs within the area illuminated by the radar beneath the satellite. A measured backscatter coefficient of these pulse returns is an indicator of the sea roughness which depends mainly on the wind speed. The strength of the return radar pulse depends on the *SWH*s sampled within the reflection area (footprint) of the pulse. In a calm sea the size of the footprint is smaller (beam footprint radius ~2km) whereas in a turbulent sea (with effective radius footprint up to 10km), where large waves prevail, the sea surface that contributes to the reflection of the radar signal increases, thus resulting in different times of return from wave crests and troughs. The satellite *SWH* measurements are necessarily carried out along the orbital ground track of satellites which are usually placed in an exact-repeat-orbit, meaning that the satellite returns almost exactly over the same location after a certain number of days (e.g. 10 days for the TOPEX/Poseidon, Jason-1 and -2 satellites, 35 days for the ERS-1, -2 and ENVISAT satellites, 90 days for the Cryosat-1 (laser altimeter) satellite, etc.). Increasing the orbital period of a satellite leads to a denser spatial coverage of the satellite's ground tracks in the sea surface, as it also does the combination of multi-mission data from several satellites with different orbital characteristics.

Local (sub-hourly, hourly or daily) time-series of *SWH* measurements can also be obtained from buoys carrying various instruments, such as sensors measuring the sea state and atmospheric conditions prevailing in the location where each buoy is moored. In the present study, one of our first tasks was to establish the expected level of confidence in the *SWH* measurements provided by satellite altimeters through relevant comparisons with respective *SWH*s from a network of buoys, as suggested by similar studies (e.g. Shanas et. al., 2014) with satisfying results. For that purpose, daily averaged buoy-observed *SWH* data were conveniently retrieved from the *Irish Weather Buoy Network* (IWBN), which provides an online data service with measurements in almost real time. Respectively, the altimeter-derived daily *SWH* data used for this comparison were obtained from the French AVISO Service, in the form of multi-satellite (Jason-1, Jason-2 and Envisat) timeseries at 1^0x1^0 grid points near each specific buoy location.

The correlation of the altimeter data with the buoy data was performed by comparing overlapping time series of the two types of *SWH* data, constructing their respective scatter plots and using appropriate indicators such as the correlation coefficient (*CC*), the bias and the root mean square error (*RMSE*) given as:

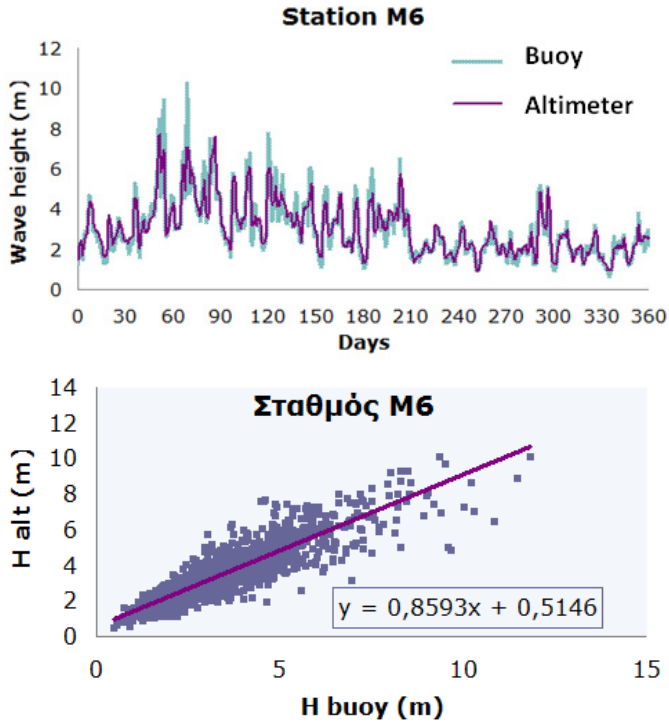

Figure 1. *At top, comparison between SWHs obtained from altimetry and from buoy measurements. At bottom, scatter plot of the comparison between altimeter data from the multi-mission AVISO product with measurements of nearest buoy.*

$$CC = \frac{\sum_{i=1}^{n}(x_i - \bar{x})(y_i - \bar{y})}{\sum_{i=1}^{n}(x_i - \bar{x})^2 \sum_{i=1}^{n}(y_i - \bar{y})^2}, \; Bias = \bar{y} - \bar{x}\,, \; RMSE = \sqrt{\frac{\sum_{i=1}^{n}(y_i - x_i)^2}{n}} \tag{6}$$

where x_i και y_i represent respectively the buoy's wave heights and the altimeter's significant wave height observations, $\bar{x}$ and $\bar{y}$ are the average daily values of the corresponding samples and n is each time series sample size.

The graphs in Figure 1 show the comparison between the time series of altimetry-derived SWHs and wave heights from the M6 station/buoy of the IWBN (top) and their corresponding scatter plot (bottom). Similar graphs were obtained for each of the remaining IWBN stations shown in Table 1. All the relevant graphs showed from a satisfactory to a very high correlation (>0.8) between the altimeter data and the buoy's data for the respective year-long time periods examined.

As shown in Table 1, the correlation coefficients CC at the five IWBN buoys range from 0.80 to 0.91, that is, values which are indicative of the strong correlation

Table 1. *Statistics of nearest grid altimeter and buoy SWH data*

Station	Location				CC	Bias	RMSE
	Buoy		Nearest altimetry grid points				
	Lat	Long	Lat	Long			
M3	51.22	-10.55	51.00	349.00	0.91	0.14	0.65
M4	55.02	-9.75	55.00	350.00	0.91	0.19	0.70
M5	51.70	-6.70	52.00	353.00	0.80	-0.18	0.66
M6	53.18	-15.73	53.00	344.00	0.90	-0.06	0.71
AMETS	54.27	-10.14	54.00	350.00	0.91	0.22	0.59

between the two types of SWH measurements at each location. The noted bias estimates range between -0.06 and 0.22 m, which in combination with the fact that the accuracy of altimeter data is generally a few centimeters, provides a further confirmation of the reliability of the altimetry-derived SWH data. The negative values of the bias error at the M5 and M6 locations indicate that the SWH being measured by the buoys, are larger than those measured by satellite altimetry, while in the remaining three locations is quite the opposite. This fact underlines the qualitatively different characteristics between the two types of measured SWH data that should be carefully taken into account in any optimization procedure (e.g. assimilation, local adaptation, etc.), and also considering that the wave height values of the altimeter data is a sampling result (i.e. an average situation wave) within the footprint of the radar pulse in the surface below the satellite, whereas the SWH values observed by the buoys have strictly local character. The noted RMSE values, in combination with the fact that the corresponding correlation coefficients are close to unity, illustrate the high degree of agreement of the time series between buoys and altimeter data measurements.

Table 2 is based on SWH measurements at the buoy station M6 and illustrates the close relation between wave period and wave height showing, in terms of SWH per meter variation and 2-sec intervals in wave period, the percentage distribution of wave sea state conditions. For this particular location, it is noted that small wave heights are associated with small wave periods and, respectively, large wave heights are associated with long periods and typically waves have heights ranging from 1 to 4 m (at 73.84% of the time) and periods from 4 to 8 s (at 82.18% of the time).

Satellite radars measure the spatial variability of wave height and wind speed with high accuracy. However, it should be noted that contrary to buoys, they do not measure the wave period which is necessary for calculating the wave power in order to estimate the wave energy potential in a given location by Equation (5). This poses the requirement to make an assumption about the dominant wave period of the prevailing waves in a given location of interest. For instance, with the altime-

Table 2. *Percentage of sea state conditions with different SWH (H_S) and wave period (T).*

Hs (m)	T (s)	t						
	0-2	2-4	4-6	6-8	8-10	10-12	12-14	Total
0-1	0.00	0.15	1.63	0.24	0.00	0.00	0.00	**2.01**
1-2	0.00	0.11	17.12	8.19	0.20	0.00	0.00	**25.62**
2-3	0.00	0.00	10.47	16.73	1.02	0.02	0.00	**28.24**
3-4	0.00	0.00	0.99	16.23	2.69	0.06	0.00	**19.98**
4-5	0.00	0.00	0.01	8.09	3.94	0.16	0.00	**12.19**
5-6	0.00	0.00	0.00	2.27	3.93	0.25	0.00	**6.46**
6-7	0.00	0.00	0.00	0.20	2.35	0.28	0.01	**2.84**
7-8	0.00	0.00	0.00	0.01	1.05	0.36	0.01	**1.42**
8-9	0.00	0.00	0.00	0.00	0.38	0.37	0.04	**0.78**
9-10	0.00	0.00	0.00	0.00	0.09	0.33	0.03	**0.45**
Total	**0.00**	**0.26**	**30.22**	**51.96**	**15.64**	**1.83**	**0.09**	**100.00**

try-derived SWH data at the grid point near the buoy station M6, this was done, on the assumption of wave periods T=1, 3, 5, 8 and 10s respectively. Figure 2 shows, at this particular location, the strong correlation that exists between the time series of the wave power per meter of wavelength as calculated from the observed buoy (SWH and wave period) data and the corresponding altimeter data on the assumption of wave period T = 8s respectively.

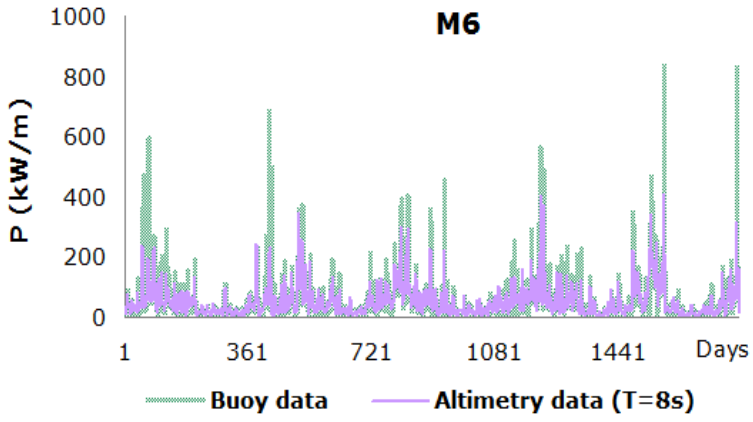

Figure 2. *Time series comparison between the wave power obtained from an altimeter (AVISO) assuming a wave period T=8s and from buoy measurements during 2009-2015.*

3. Spatial and Temporal Analysis Results

3.1. General statistics and trends

For a time span of nearly 6 years, during the period 2009-2015, gridded observational records of satellite altimetry-derived SWH and wind speed modulus in two testing areas surrounding the maritime regions of Greece and Cyprus were extracted from the AVISO Service. Such observations for SWH are produced by merging all available relevant data provided by various altimetry satellites. Based on these data, various statistical measures relating to the temporal (monthly and seasonal) and/or spatial variations of wave power and wave energy density were obtained. The locations of interest shown in Figure 3 were selected by examining (a) known patterns of dominant wind directions, (b) considering the stipulated levels of wave power based on similar studies and/or (c) representative areas with relatively high productivity of the marine environment (e.g. fisheries, aquaculture).

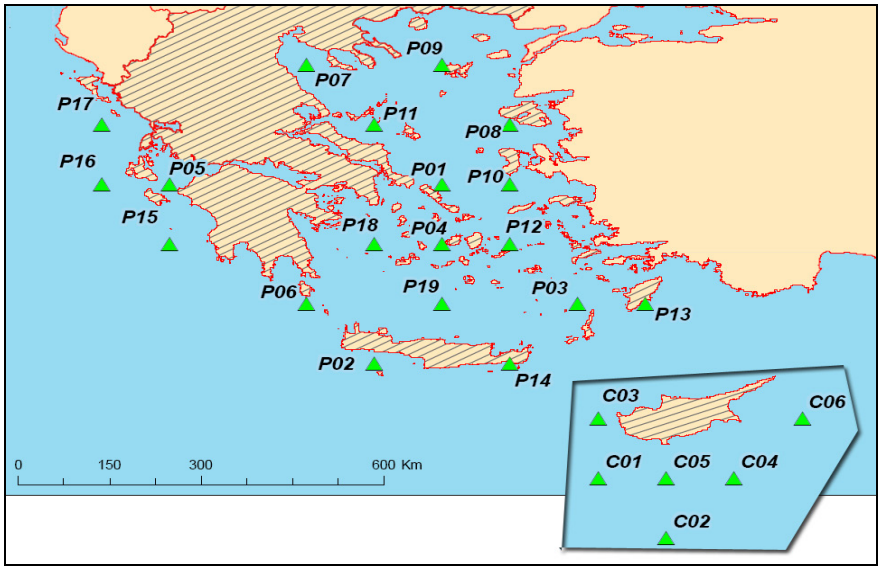

***Figure 3**. Selected test locations in Eastern Mediterranean.*

Full statistical results regarding the wave conditions in each of the selected locations were presented by Kaselimi (2015). Overall, the wave statistics obtained for Greece indicated that the average SWH among those locations varied from 0.80m to 1.10m with extreme values ranging from a few centimeters to about 4m. Generally, wave conditions of SWH greater than 1m appear with a 30-45% frequency. As shown in Table 3, the most intense conditions can be found in the areas of Gavdos (P02), Kythera (P06) and Koufonisia (P14), whereas the lowest wave conditions are noted around Skopelos (P11), Lesvos (P08) and Limnos (P09).

Table 3. *Descriptive statistics obtained for altimetry-derived SWH for sample locations exhibiting high and low wave conditions*

Hs (m)	P02 Gavdos	P06 Kithira	P14 Koufonisia	…	P11 Skopelos	P08 Lesvos	P09 Limnos
Days	1935	1911	1929	…	1925	1877	1885
Mean	1,10	1,06	1,07	…	0,86	0,83	0,83
St Dev	0,56	0,55	0,54	…	0,49	0,51	0,52
Min	0,14	0,12	0,09	…	0,01	-0,10	-0,15
Q1	0,70	0,66	0,69	…	0,50	0,48	0,46
Median	0,97	0,94	0,94	…	0,75	0,71	0,71
Q3	1,40	1,34	1,33	…	1,10	1,07	1,08
Max	3,87	3,96	3,54	…	3,47	4,05	3,95
%(Hs>1m)	48	45	46	…	30	29	29

Similar statistical results for the locations around Cyprus show that the mean SWH values are around 0.95m, with extreme values ranging from a few centimeters to about 4.5m. The most intense wave conditions are displayed offshore Paphos (C01) where the mean SWH during the same period is 0.98m, while in all other locations the average SWH were very similar (between 0.89m and 0.97m).

From the same data, for each location, we have obtained graphs of (rolling or running) SWH moving averages, as shown in Figure 4, for instance, for Gavdos (P02) and Paphos (C01). SWH moving averages are usually used to illustrate the typical wave conditions within a specified duration by smoothing out short-term fluctuations and thus highlight long-term trends or cycles of the prevailing wave conditions (e.g. the existence of inter-annual variability).

It is well established that complex meteorological phenomena and geographical features occurring in the Eastern Mediterranean induce large wind variability causing strong spatial and temporal variability in the wave conditions. Characteristically, Queffeulou and Bentamy (2007) have shown that the areas south of Crete and Rhodes and around Cyprus are dominated by relatively high mean SWH during the summer months. For instance, the strong sea state in the Aegean Sea is produced by the southerly extension, between Rhodes and Crete, resulting in the northern monsoon-type yearly seasonal winds (the so-called '*meltemia*' or '*etesian*'), whose maximum strength and occurrence is encountered in the months of July and August. In the present study, by dividing the available data in annual intervals, we examined the effects of seasonality in all points of interest, so that to check how those phenomena affect wave conditions and also to gain a complete and detailed picture of the variability of wave conditions. The aggregated annual diagrams in Figure 5 represent the average SWH values per month and the mean

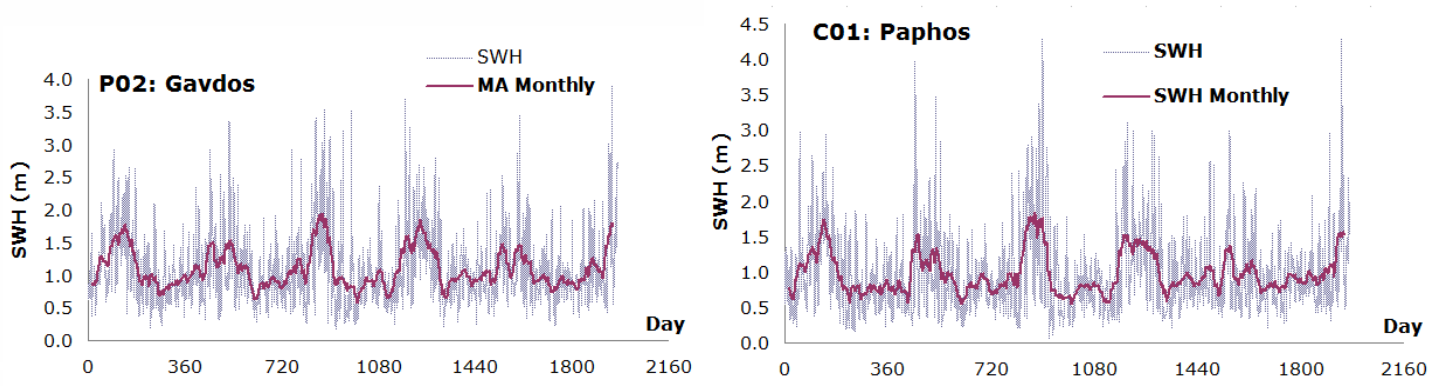

Figure 4. *Time series of significant wave height (H_S) and moving average for a window of 31 days during 2009-2015.*

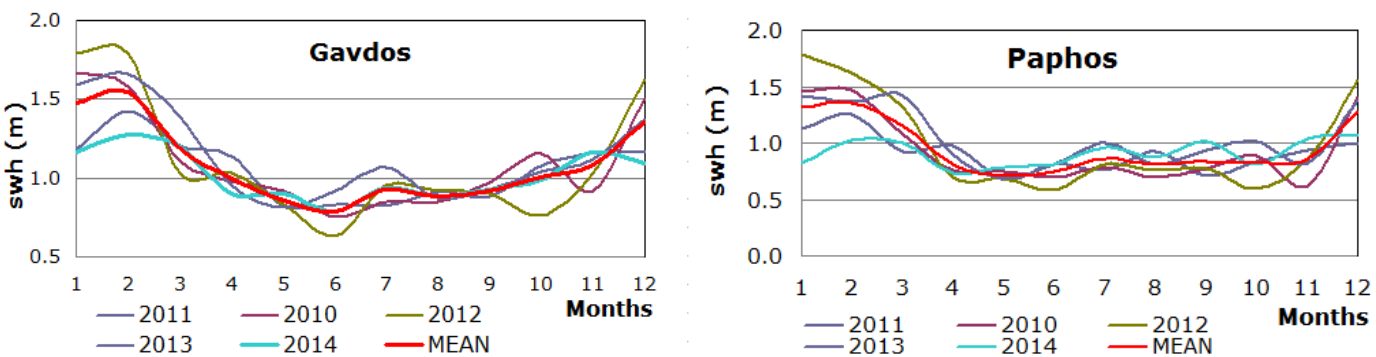

Figure 5. *Mean annual cycle for SWH conditions in Gavdos and Paphos.*

annual cycle near Gavdos and Paphos. In both locations, maximum SWH values are reached during January and February, followed by a significant reduction in magnitude during spring, and a period of sustainability during summer. Between the two locations, during July the phenomenon due to the etesian winds is immediately noticeable, albeit is more intense in Gavdos and less so in Paphos.

The Mediterranean Sea, just as the Baltic Sea and the North Sea in Europe's northern latitudes, as well as some regions closer to the equator, has sheltered waters and calmer regional seas exhibiting a milder, steady wave climate, but still posses a large portion of the world's exploitable wave energy potential. Existing practical experience to date suggests that when taking into account technical and economic constraints, near-shore, steady sea state areas offer far more attractive opportunities for exploitation of the wave energy than other oceanic deep-water areas, whereby waves can travel in almost any direction, making energy extraction more difficult. In contrast, near-shore locations provide only slightly fewer exploitable resources, but with far less extreme sea states, easier access and significantly easier design criteria and operating conditions for deploying wave energy converter installations. This, in turn, results in far lower cost and investment requirements per MW of generating power capacity. Therefore, one of the issues often considered when choosing the location of a wave farm is the existence of steady wave conditions that will ensure the proper operation of a wave farm. In the present study, the long-term (2009 to 2015) variation of the wave conditions was studied using linear regression models. For instance, the respective linear function trendlines were estimated as $y = 0.002x + 1.730$ for Gavdos and as $y = 0.001x + 1.599$ for Paphos, indicating mild nearly steady state (or very small growing) wave conditions over the 6-year period studied. In these linear regression equations y denotes SWH levels and x is the number of months since the beginning of the period studied.

3.2. Spatial distribition of wave power

The next important stage in evaluation of wave energy potential is concerning spatial distribution of wave power. As already mentioned, the quantitative index of wave power P, as given by Equation (5), depends on significant wave height (H_s) and the period T. Emmanouil et al. (2015) in a comprehensive study for the Greek seas, and Zodiatis et al. (2014) for a similar study for Cyprus have used wave periods derived from the WAM model in an effort to construct maps of the spatial distribution of wave power P for these regions. In the present study, relevant statistics for wave power were estimated from altimetric SWHs using periods T = 1, 3, 5, 8 and 10s respectively. The wave power map shown in Figure 6 was constructed using 6 years of available altimetry-derived SWH observations for 2009-2015 and assuming a wave period T = 5s.

Clearly, from the various aspects examined in the present wave data analysis, it is

concluded that areas with high enough levels of wave energy potential can be found in the south side of Crete for Greek area and the area around Paphos in Cyprus, where wave conditions are considered mild but stable, with regularly occurring wave climate. In the area of Crete wave power amounts on average at the level of about 4 KW/m and respectively in Paphos at 2 KW/m. These levels, while being considered moderate in size, they are exploitable and even favorable, in terms of other criteria such as a robust WEC structure which can be constructed within selected locations in order to ensure optimal functionality in wide range of conditions and survivability, as well as taking advantage of operational characteristics such as wave overtopping and run-up. Thus, utilization of existing wave energy potential requires appropriate energy conversion systems so as to reduce the costs related to the establishment and the operation of such devices, so that the amount of energy that could be generated would be exploitable and capable to offer practical solutions to current energy problems in these areas.

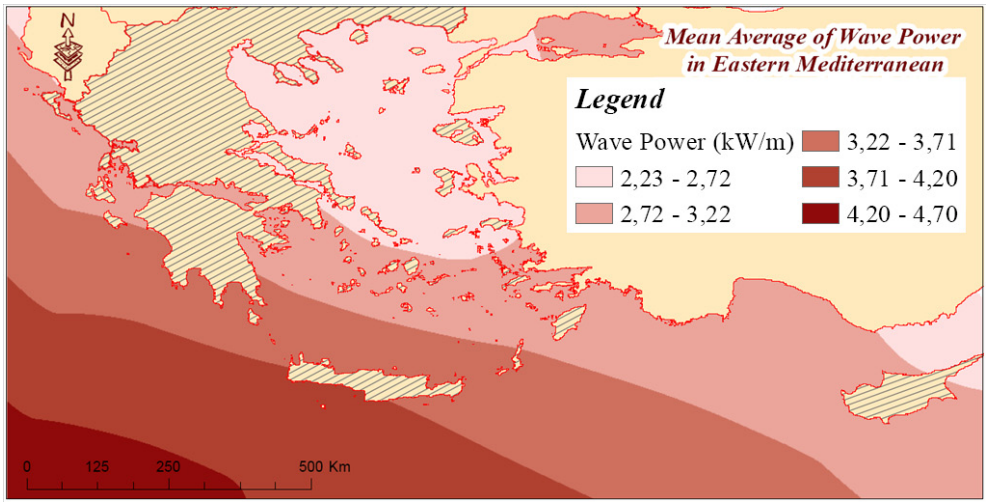

***Figure 6**. Mean average of wave power.*

3.3. Installation of wave farms

In practice, the wave power produced by a wave energy converter is less than the theoretically available due to the prevailing local wave conditions. Among crucial constraints, the direction of upcoming waves is included, as most WECs utilize only waves whose upcoming front is properly oriented to the dominant direction which is required by each converter. Thus, the average incident power, as shown in the flowchart of Figure 7, is a function related to the average wave power and its value depends on the diameter of the point absorber type WEC (e.g. D = 10 m) and a reduction factor DF which is called *directivity factor*, and in this study taken as equal to 0.9. The effectiveness with which a particular WEC device captures wave

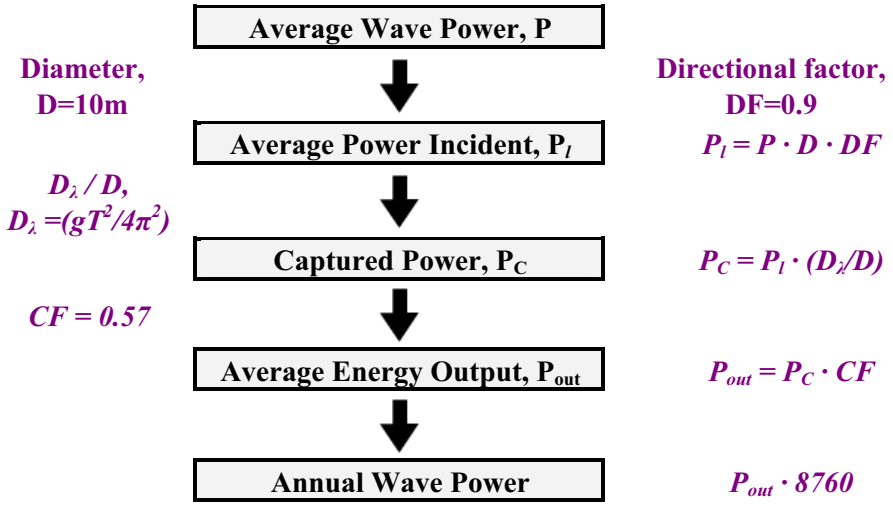

Figure 7. *Wave power estimation steps*

energy is a function of the sea state. The captured power by a WEC absorber is theoretically calculated and depends on the length D_λ of the upcoming wave which, in turn, depends on the wave period T. In practice, during operation, there will be periods of reduced output due to faults and maintenance which has a possible impact on electricity production. Finally, the average technically feasible energy output P_{out} is calculated as a percentage of captured power depending on efficiency factor, conservatively taken, in this study, as $CF = 0.57$. The main advantage of an array of point absorbers, such as shown in Figure 8, is that they can absorb much more wave energy, producing large amounts of electricity even in seas that are characterized by mild but also steady wave conditions. Moreover, the idea of symmetrical hexagonal arrangement of devices (Figure 8, right) is introduced so that the device can be independent from the prevailing direction of the waves and consequently most of the upcoming waves can be exploited (regardless of their direction). Calculating energy for a simplest model of an array of point absorbers, requires to take into account that buoys at the back of the array will receive less energy than those at the front of a wave field in a predominant direction. However, a suitable distance between each buoy could maintain the absorption of energy in each row at a level of 2% or less.

Similarly, in a system where a number of arrays of point absorbers are deployed over a wide marine area, the arrays closest to upcoming waves will receive more energy, contrary to the ones behind them in a predominant direction. However, this additional shadowing effect can be avoided through an ample distance so that the ripples can be renewed with the aid of the wind and recover the original size and their initial wave power. By positioning the WEC devices in columns perpendicular to the prevailing wind direction and forming a larger rectangular array, the dis-

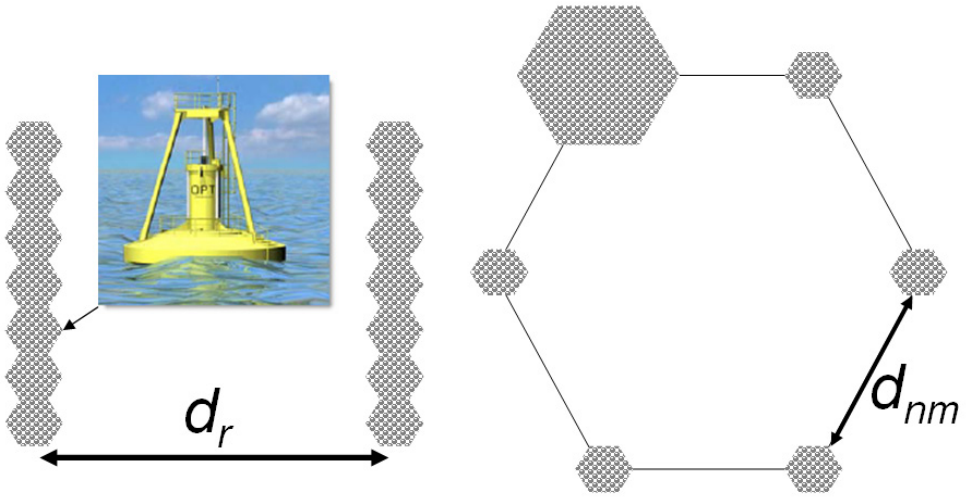

Figure 8. *Schematic arrangement of WEC wave absorbers to form a suitable wave farm (after Bernhoff et al, 2006).*

tance required to restore wave height is calculated using the relationship between the significant wave height H_s, the wind speed V and the length of the fetch F (Bernhoff et al., 2006),

$$H_s = \frac{0.91\, V^{1.175}\ F^{0.41}}{1000} \tag{7}$$

Equation (7) is used for rectangular arrays of point absorbers. Quoting the example from Bernhoff et al. (2006), an initial value of SWH=2m will be reduced to 1.7m, while the wave is penetrating the first column of the devices. For a wind speed of 10 m/s the required fetch F, so that wave height can reach 2m in deep water, is 190 km. Correspondingly, the fetch of the wave for significant wave height of 1.7 m is about 130 km. Thus, theoretically, attenuated waves require an inter-row distance d_r equal to 60 km (= 190 km-130 km), so as to recover their initial wave height (from 1.7 m to 2 m, which was originally). With a typical diameter of a WEC array, equal to 600m, the extent required to recover the wave height is 36 km^2 per array which corresponds to a distance between the nearest neighbor WEC absorber equal to d_{nm} = 4.5 km.

Summarizing the results of the current study, and also presented in full by Kaselimi (2015), revealed that, in Greece, the largest wave heights and therefore higher levels of wave power are to be found (in descending order) around the locations P02 (Gavdos), P14 (Koufonisia), P06 (Kythira), P15 (Peloponnese-Messenia), P19 (Santorini), P16 (Kefalonia), P03 (Karpathos), P05 (Zakynthos) and P13 (Rhodes). Currently, Gavdos, Koufonisia, Santorini, Rhodes and Karpathos, in terms of the existing power grid system, are non-interconnected islands, that is to say, are

Table 4. *Levels of energy demands from current stand-alone power systems in Greek islands and the total energy that each wave farm can produce.*

Stand-alone power system	Island		2008	2009	2010	2011	2012	2013	x85 point absorbers (MWh)	x7 arrays of point absorbers (GWh)
Gavdos	Gavdos	Demand (MWh)	279	280	355	428	486	471	8202	57.4
		Peak (kW)	73	81	94	95	148	115		
Paros	Paros	Demand (MWh)	202835	205300	208206	207254	203622	194740	7717	54
	Naxos									
	Antiparos									
	Koufonisia									
	Sxoinousa									
	Hrakleia	Peak (kW)	63100	60410	71100	61600	63300	62400		
	Skinos									
	Folegandros									
	Ios									
Thira	Thira	Demand (MWh)	112520	117161	117957	120057	120817	120199	7085	49.6
	Thirasia	Peak (kW)	34100	31700	36400	33550	35800	32500		
Karpathos	Karpathos	Demand (MWh)	35234	37094	37829	38784	38985	36931	6715	47
	Kasos	Peak (kW)	9900	9800	11400	10900	11780	11010		
Rodos	Rodos	Demand (MWh)	757788	763790	764438	780413	790593	760658	6631	46.4
	Xalki	Peak (kW)	200000	194800	206000	194000	211800	188500		

largely served by autonomous oil-fuel and diesel-electric generators, which generate significant pollutants, and their electricity generation cost is extremely high due to the utilization of outdated autonomous power stations. The actual energy demands for these islands are presented in Table 4 (as extracted from data by Greece's Regulatory Authority for Energy, cf. http://www.rae.gr/site/categories_new/electricity/market/mdn.csp), together with the respective estimated levels of energy that could potentially be made available if suitable wave parks were to be utilized in these areas. Similarly, in the marine area of Cyprus where more energy is expected to be produced are in the locations C01 and C02, where suitable wave farms could produce some 48 GWh in each location.

Conclusion

From the current detailed analysis of long-term SWH data derived from multiple altimeter satellites, it is confirmed that the Eastern Mediterranean has significant exploitable wave energy potential, especially within the maritime regions of southwestern Aegean and the western and southern sea areas of Cyprus. These areas display the highest levels of the Mediterranean, while having favorable low annual variability, but also stable, as well as small exposure to extreme sea state conditions that can lead to weak performance.

Such exploitation of wave energy potential, albeit at smaller levels than those, for instance, along the Atlantic coast or the northern European seas, could meet a significant proportion of the energy needs of the many islands in this region. Evidently, the areas examined in this study offer a clear example that given time and with the right governmental support, wave energy can progress along the innovation chain towards commercial viability and easier adaptation to large power grids. Therefore, as a next step, it would be prudent to initiate further efforts leading towards practical demonstration of innovative, cost efficient and environmentally benign offshore renewable energy conversion platforms for wave energy resources in these areas.

References

Ayat, B., 2013. Wave power atlas of Eastern Mediterranean and Aegean Seas. *Journal of Energy* 54. 251-262.

Bernhoff, H., Sjöstedt, E., Leijon, M., 2006. Wave energy resources in sheltered sea areas: A case study of the Baltic Sea. *J. of Renewable Energy* 31. 2164–2170.

Clement, A., McCullen, P., Falcão, A., Fiorentino, A., Gardner, F., Hammarlund, K., Lemonis, G., Lewis, T., Nielsen, K., Petroncini, S., Pontes, M. T., Schild, P., Sjostrom, O. B., Sørensen, C. H., Thorpe, T., 2002. Wave energy in Europe: current status and

perspectives. *J. of Renewable and Sustainable Energy Reviews* 6. 405-431.

Delikaraoglou, D. and S. Delikaraoglou, 2012. The contribution of geodetic altimeter satellites in mapping the Greek area: a feasibility study for the exploitation of the wave energy (in Greek). *GEOGRAFIES* 19, pp. 70-88. Available at: http://geographies.gr/wp-content/uploads/2013/05/GEO19-070-088_new.pdf.

Emmanouil, G., Galanis, G., Kallos, G., Zodiatis, G., Kalogeri, C., 2015. Wind-Wave energy potential over the Greek seas. *In: EWEA Offshore conference, Copenhagen*, 2010.

Falcão, A., 2010. Wave energy utilization: A review of the technologies. *J. of Renewable and Sustainable Energy Reviews* 14. 899–918.

Iglesias, G., Carballo, R., 2011. Choosing the site for the first wave farm in a region: A case study in the Galician Southwest (Spain). *J. of Energy* 36. 5525-5531.

Kaselimi, M., 2015. An analysis of multi-mission satellite altimeter data for estimating the prospects of wave energy potential in Eastern Mediterranean (in Greek). Diploma Thesis, Department of Surveying Engineering, National Technical University of Athens. Available at: http://publicationslist.org/php/publist.php?u=maria.kaselimi&t=85#refid85.

Pontes, M. T., Athanassoulis, G. A., Barstow, S., Cavaleri, L., Holmes, B., Mollison, D., and Oliveira Pires, H., 1996. WERATLAS-Atlas of Wave Energy Resource in Europe. Technical Report, DGXII Contract No. JOU2-CT93-0390, INETI, Lisbon.

Queffeulou, P., Bentamy, A., 2007. Analysis of Wave Height Variability Using Altimeter Measurements: Application to the Mediterranean Sea. *J. of Atmospheric and Oceanic Technology* 24. 2078-2092.

Shanas, P. R., Sanil Kumar, V., Hithin N. K., 2014. Comparison of gridded multi-mission and along-track mono-mission satellite altimetry wave heights with in situ near-shore buoy data. *J. of Ocean Engineering* 83. 24-35.

Soukissian, T.H., Prospathopoulos, A.M., 2003. Implementation of the 3rd Generation Wave Model WAM-Cycle 4 in Aegean Sea (in Greek). Tech. Chron. Sci. J., IV, No 1-2. pp. 7-19.

Zodiatis, G., Galanis, G., Nikolaidis, A., Kalogeri, C., Hayes, D., Georgiou, C. G., Chu, C. P., Kallos, G., 2014. Wave energy potential in the Eastern Mediterranean Levantine Basin. An integrated 10-year study. *J. of Renewable Energy* 69. 311-323.